Wiley Online Library
Early View publication on www.wileyonlinelibrary.com
(issue and page numbers not yet assigned;
citable using Digital Object Identifier – **DOI**)

Phys. Status Solidi B, 1–4 (2014) / **DOI** 10.1002/pssb.201451224

physica status solidi b
www.pss-b.com
basic solid state physics

Electron spin lifetime in chemically synthesized graphene sheets

Bálint Náfrádi*,[1], László Forró[1], and Mohammad Choucair,[2]**

[1] Institute of Physics of Complex Matter, EPFL, Lausanne, Switzerland
[2] School of Chemistry, University of Sydney, Sydney 2006, Australia

Received 8 May 2014, revised 11 September 2014, accepted 26 September 2014
Published online 2 November 2014

Keywords electron spin resonance, gas sensing, graphene, spintronics

* Corresponding author: e-mail nafradi@yahoo.com, Phone: +41 21 693 4515, Fax: +41 21 693 4470
** e-mail mohammad.choucair@sydney.edu.au, Phone: +61 2 9351 5843, Fax: +61 2 9351 3329

Graphene is theoretically expected to be a highly suitable material for spintronic and quantum computation applications. Current experimental reports assign surprisingly low spin lifetimes to graphene and related carbon structures. Recently, we showed a solvothermal synthesis method that can be employed to produce a high-purity sample, which approximates very well the assembly of graphene sheets. Using the contactless spectroscopic technique of electron spin resonance (ESR), we were able to identify in this graphene material the ESR of both conduction electrons and localized spins [Náfrádi et al., Carbon **74**, 346–351 (2014)]. Here, we show the temperature dependent evolution of the ESR of these two spin species.

1 Introduction A material with long spin relaxation time, T_S, permits the manipulation of coherent spin states and thus allows its utility in spintronics applications. Graphene has been suggested as a promising material for spintronics applications due to the long T_S expected from the weak hyperfine interactions due to the absence of nuclear spins for the main ^{12}C isotope and due to the small spin–orbit coupling of the light carbon atoms. However, values of T_S have been reported in the limited 0.2–2.3 ns range [2–6] based on spin transport experiments. The origin of the surprisingly low experimental spin lifetime is under intensive debate. It was proposed that the sample preparation has an important effect on the measured T_S [2]. Alternative scenarios suggested the effect of the substrate [7], impurities [8, 9], finite-sized flakes [10, 11], or ripples [12–14] to explain the unexpectedly small T_S found in graphene. Contactless experimental methods to determinate the intrinsic spin lifetime are thus favorable because impurity and substrate effects can be avoided.

Electron spin resonance (ESR) is a sensitive contactless method for measuring T_S [1, 15–19]. In carbon-based insulating systems, the spectroscopic information due to the small spin–orbit coupling and thus g-factor anisotropy is sometimes limited [20–24]. This difficulty can be overcome by using high-frequency ESR methods since the spectral resolution is proportional to the ESR frequency in paramagnetic samples [25–30]. Moreover, in the case of metallic systems, the separation of localized and itinerant moments is feasible by ESR [31–35].

Here, we report on multi-frequency ESR spectroscopy on a chemically synthesized graphenic material, which mimics the assembly of uncoupled graphene sheets. In this high purity material, a surprisingly long spin lifetime of 65 ns was found for itinerant conduction electrons.

2 Experimental We employed a solvothermal synthesis method to obtain the graphene material. This procedure produces three-dimensional networks of graphene [1, 36]. As alcohol feedstock, propanol was used. The solvothermal reaction was performed with sodium metal at 493 K for 72 h. A solid product was obtained by the solvothermal reaction, which was rapidly pyrolized. The resulting carbon material was subsequently washed with water and with acidified ethanol (2 M hydrochloric acid in ethanol, 1:4 v/v ratio). Finally, the product was filtered under dynamic vacuum before drying in a vacuum oven at 473 K for 1 h.

Multi-frequency ESR spectroscopy in the 9.4–420 GHz frequency-range was performed. The temperature was changed in the 2–300 K temperature intervals. At the lowest 9.4 GHz frequency, a commercial ESR spectrometer was used. In the millimetre wave range (105–420 GHz) experiments were carried out on a home-made quasi optical

spectrometer [37, 38]. In order to enhance sensitivity, conventional first-derivative-absorption spectra were detected through applying sinusoidal modulation of the externally applied magnetic field and lock-in detection. In order to avoid distortion of the detected spectral lines the incident microwave powers as well as the magnetic field modulation amplitude were reduced. The spectroscopic parameters, i.e., the ESR linewidth (ΔH), g-factor, and spin susceptibility (χ), were obtained by least square fitting of the derivative absorption spectra. The absolute value of χ was determined by a calibrated $CuSO_4 \cdot 5H_2O$ reference sample following calculations detailed in Ref. [39].

3 Results and discussion Washing the graphene material by stirring, and mild sonication treatments, are known to disrupt the weakly fused graphene structure to obtain free sheets [40]. Indeed, transmission electron microscopy (TEM) in Fig. 1 shows that the secondary structure of the material is dominated by extended networks of fused graphene sheets. These large fragmented sections spanning micrometer length scales [1]. From direct observation of Moiré patterns under the TEM, we realize that our sample consists of layers of graphene with a small degree of angular offset (i.e., twisting) with no inter-planar correlation. Selected region electron diffraction pattern showed, however, that the graphene material consists of large in-plane hexagonal domains. Moreover, primary graphitic feature, i.e., the ABAB stacking was absent.

Low-frequency ESR at 9.4 GHz revealed a single highly symmetric Lorentzian signal of the graphenic material at room temperature. The line is at $g = 2.0044$ position with $\Delta H = 0.046$ mT linewidth (Fig. 2). The spin susceptibility is $\chi = 7 \times 10^{-8}$ emu g^{-1}. Assuming that magnetization originates only from spin-1/2 paramagnetic moments this value translates to $\chi = 3.7 \times 10^{19}$ spin g^{-1} [1]. The corresponding average spin–spin distance is $r_{e\text{-}e} = 1.3$ nm assuming non-correlated defect sites and uniform three-dimensional distribution for defects. Remarkably, the dipole–dipole interaction between nearest neighbor spins with this $r_{e\text{-}e}$ would induce an ESR linewidth of $\Delta H_{dip\text{-}dip} = 0.87$ mT [1, 41]. This corresponding linewidth is about 20 times broader than the experimentally observed one. Assuming two-dimensional spin distribution the dipole–dipole linewidth would be even greater. Moreover, the dipole–dipole interaction is only a lower bound for the ESR linewidth. In insulating carbon nanostructures unresolved hyperfine interactions and other anisotropies, like g-factor anisotropy, in principle, further broadens the line [42, 43]. Thus, a narrowing mechanism is required to be active in the system to describe the observed externally narrow ESR linewidth. There are two possible processes: motional narrowing of itinerant electrons or exchange narrowing between localized spins. In insulting system exchange-

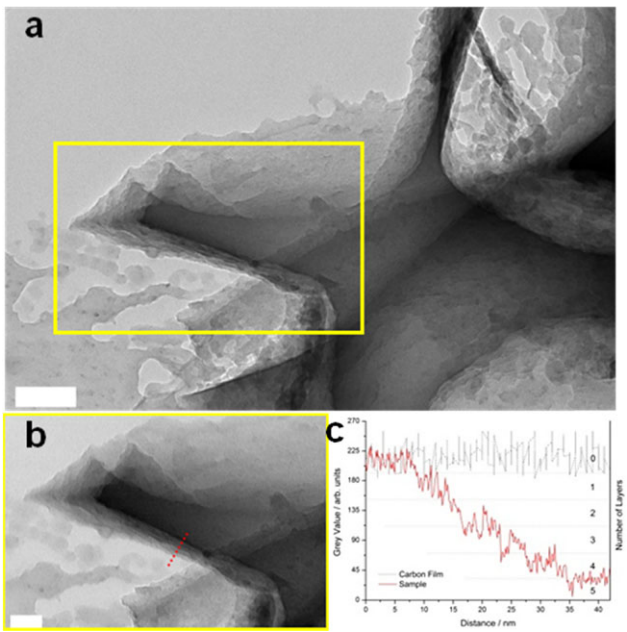

Figure 1 TEM of an X-shaped graphene region with the yellow box highlighting an area shown in (b) emphasizing a layered structure. The graphene material forms narrow junctions between 20 and 80 nm in width, which meet at an island ca. 250 nm × 250 nm in size. The graphene canopy is evident both on top and beneath the extended network, verging on decomposition due to the intensity of the beam. (c) The differences in opacity of the layered material was plotted by taking the line profile shown in (b) across the fringes formed in the image of the graphene material over the substrate, which indicated the approximate number of sheets to be greater than 5. The abscissa in (c) is the length of the contrast profile taken across the region in the image from the substrate over a region of the sample with no consideration for depth. Scale bars represent in (a) 100 nm and (b) 50 nm.

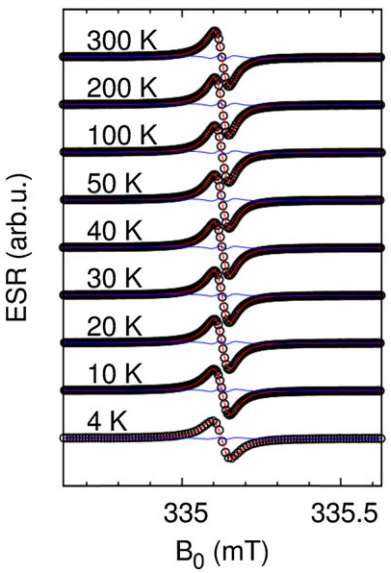

Figure 2 ESR spectra (9.4 GHz) measured at various temperatures between 4 and 300 K (points). Red lines through the points are the result of a fit to a derivative Lorentzian function. The quality of the fit is good shown by the residue line (blue).

narrowing between paramagnetic defects could be expected. However, due to the large $r_{e\text{-}e}$, this interaction can be excluded in our case. Thus, we left with the conclusion that itinerant conduction electrons are playing a crucial role in the observed narrowing of the ESR linewidth.

In order to further support the presence of conduction electrons, we compare ESR spectra taken at various temperatures at 9.4 GHz (Fig. 2) and 315 GHz (Fig. 3). At 9.4 GHz, a single Lorentzian line persists at all temperatures. The width slightly decreases upon cooling and reaches a minimum of $\Delta H = 0.41$ mT at around $T = 100$ K. By further cooling the sample, ΔH starts to increase and $\Delta H = 0.49$ mT is reached at $T = 5$ K. In this low-temperature range, however, the deviations from the Lorentzian shape are growing.

In contrast to 9.4 GHz ESR, experiments at 315 GHz clearly show the presence of itinerant and localized spins (Fig. 3). At high temperatures, a single Lorenztian line is observed similar to the 9.4 GHz case. Only the line distortion is somewhat higher. At low temperatures, however, a spectrum characteristic to powdered material gradually develops with extremely small g-factor anisotropy. Below 50 K, the spectra change drastically. A powder distribution spectrum is clearly observable furthermore, a new line with conduction electron spin resonance (CESR) properties appears in the 315 GHz spectra (Fig. 3).

At low temperatures, a paramagnetic powder-distribution spectrum is perfectly described with $g_{xx} = 2.00441$, $g_{yy} = 2.00452$, $g_{zz} = 2.00431$ g-factor parameters. The isotropic CESR line with $g_{CESR} = 2.00434$ is also observable simultaneously.

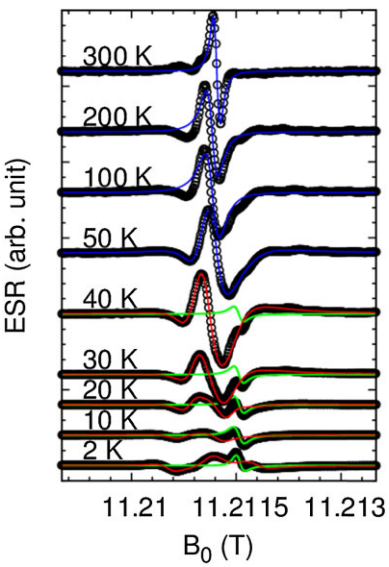

Figure 3 ESR spectra (315 GHz) at various temperatures between 2 and 300 K (points). The blue lines tracing fits to a Lorentzian profile. Below 40 K fits to the narrow CESR line shown in green and paramagnetic powder spectra shown in red. Intensity is scaled to the CESR intensity at low temperatures. Above 50 K, the peak-to-peak amplitude of the paramagnetic signal is normalized.

The gradual broadening of the paramagnetic line above 50 K and a smooth development of the powder-distribution spectra is the consequence of the gradual decoupling of itinerant and localized spins. The resolved extremely small g-factor anisotropy, $\Delta g = 0.00021$, produces about 0.035 mT linewidth at 9.4 GHz in accordance with the observed low temperature broadening at 9.4 GHz [1]. The spin susceptibility of the CESR line at 315 GHz is about 8% relative to the paramagnetic signal, which is in good agreement with the 9.4 GHz susceptibility anomaly [1]. The line we assigned to CESR based on the 315 GHz experiments exhibits temperature independent linewidth, g-factor, and susceptibility. These are the well-known benchmarks of a metallic signal. Note that the apparent increase of the CESR amplitude (green line in Fig. 3) relative to the paramagnetic powder line (red line in Fig. 3) at low temperatures is a result of spectral broadening of the paramagnetic line. The susceptibility associated to the CESR is temperature independent. Remarkably, ΔH_{CESR} observed below 50 K yields 65 ns spin lifetimes while assuming that the linewidth is homogeneous, i.e., spin–spin and spin–lattice relaxation times are equal ($T_1 = T_2$) [1, 44]. To further clarify this statement, however, additional pulsed ESR experiments are required.

4 Conclusions Our results have provided new insights into the interactions between localized and itinerant electros in chemically derived graphene. We found a single averaged ESR line at high temperatures and low frequencies originating from a motionally averaged ESR of localized and itinerant electrons. The independent ESR of two spin centers can be resolved at high frequencies and low temperatures to reveal independently the paramagnetic and CESR contributions. The results highlight the important role of itinerant conduction electrons in the spin dynamics of graphene systems. From our results, the spin lifetime based on the low-temperature ESR linewidth of the CESR ($\Delta H_{CESR} = 0.14$ mT) was found to be 65 ns [1, 42, 45]. This is in the range suitable for spintronics applications.

Acknowledgements M. C. acknowledges financial support from The University of Sydney and technical assistance from the Australian Centre for Microscopy and Microanalysis. Work at Lausanne was supported by the Swiss National Science Foundation.

References

[1] B. Náfrádi, M. Choucair, and L. Forró, Carbon **74**, 346–351 (2014).
[2] B. Dlubak, M.-B. Martin, C. Deranlot, B. Servet, S. Xavier, R. Mattana, M. Sprinkle, C. Berger, W. A. De Heer, F. Petroff, A. Anane, P. Seneor, and A. Fert, Nature Phys. **8**, 557–556 (2012).
[3] N. Tombros, C. Jozsa, M. Popinciuc, H. T. Jonkman, and B. J. van Wees, Nature **448**, 571–574 (2007).
[4] R. G. Mani, J. Hankinson, C. Berger, and W. A. de Heer, Nature Commun. **3**, 996 (2012).
[5] S. Krompiewski, Nanotechnology **23**, 135203 (2012).

[6] M. Gmitra, S. Konschuh, C. Ertler, C. Ambrosch-Draxl, and J. Fabian, Phys. Rev. B **80**, 235431 (2009).
[7] H. Castro Neto and F. Guinea, Phys. Rev. Lett. **103**, 026804 (2009).
[8] C. Jozsa, T. Maassen, M. Popinciuc, P. J. Zomer, A. Veligura, H. T. Jonkman, and B. J. van Wees, Phys. Rev. B **80**, 241403 (2009).
[9] W. H. Wang, K. Pi, Y. Li, Y. F. Chiang, P. Wei, J. Shi, and R. K. Kawakami, Phys. Rev. B **77**, 020402 (2008).
[10] M. Popinciuc, C. Jozsa, P. J. Zomer, N. Tombros, A. Veligura, H. T. Jonkman, and B. J. van Wees, Phys. Rev. B **80**, 214427 (2009).
[11] L. Tapaszto, T. Dumitrica, S. J. Kim, P. Nemes-Incze, C. Hwang, and L. P. Biro, Nature Phys. **8**, 739 (2012).
[12] V. K. Dugaev, E. Y. Sherman, and J. Barnaś, Phys. Rev. B **83**, 085306 (2011).
[13] D. Huertas-Hernando, F. Guinea, and A. Brataas, Phys. Rev. Lett. **103**, 146801 (2009).
[14] W. Han, K. Pi, K. M. McCreary, Y. Li, J. J. I. Wong, A. G. Swartz, and R. K. Kawakami, Phys. Rev. Lett. **105**, 167202 (2010).
[15] B. Náfrádi, N. M. Nemes, T. Fehér, L. Forró, Y. Kim, J. E. Fischer, D. E. Luzzi, and F. Simon, Phys. Status Solidi B **243**, 3106–3110 (2006).
[16] F. Simon, H. Kuzmany, B. Náfrádi, T. Fehér, L. Forró, F. Fülop, A. Jánossy, L. Korecz, A. Rockenbauer, F. Hauke, and A. Hirsch, Phys. Rev. Lett. **97**, 136801 (2006).
[17] L. Mihály, T. Fehér, B. Dóra, B. Náfrádi, H. Berger, and L. Forró, Phys. Rev. B **74**, 174403 (2006).
[18] F. Simon, D. Quintavalle, A. Jánossy, B. Náfrádi, L. Forró, H. Kuzmany, F. Hauke, A. Hirsch, J. Mende, and M. Mehring, Phys. Status Solidi B **244**, 3885–3889 (2007).
[19] D. V. Konarev, S. S. Khasanov, A. Y. Kovalevsky, D. V. Lopatin, V. V. Rodaev, G. Saito, B. Náfrádi, L. Forró, and R. N. Lyubovskaya, Cryst. Growth Des. **8**, 1161–1172 (2008).
[20] S. Toth, D. Quintavalle, B. Nafradi, L. Forro, L. Korecz, A. Rockenbauer, T. Kalai, K. Hideg, and F. Simon, Phys. Status Solidi B **245**(10), 2034–2037 (2008).
[21] S. Toth, D. Quintavalle, B. Nafradi, L. Korecz, L. Forro, and F. Simon, Phys. Rev. B **77**(21), 214409 (2008).
[22] F. Simon, M. Galambos, D. Quintavalle, B. Nafradi, L. Forro, J. Koltai, V. Zolyomi, J. Kurti, N. M. Nemes, M. H. Rummeli, H. Kuzmany, and T. Pichler, Phys. Status Solidi B **245**(10), 1975–1978 (2008).
[23] A. Olariu, B. Nafradi, L. Ciric, N. M. Nemes, and L. Forro, Phys. Status Solidi B **245**(10), 2029–2033 (2008).
[24] L. Ciric, K. Pierzchala, A. Sienkiewicz, A. Magrez, B. Náfrádi, D. Alexander, J. Warner, H. Shinohara, M. H. Ruemmeli, T. Pichler, G. Andrew, D. Briggs, and L. Forró, Phys. Status Solidi B **245**(10), 2042–2046 (2008).
[25] L. Ciric, A. Sienkiewicz, B. Náfrádi, M. Mionic, A. Magrez, and L. Forró, Phys. Status Solidi B **246**, 2558–2561 (2009).
[26] Á. Antal, T. Fehér, B. Náfrádi, R. Gaál, L. Forró, and A. Jánossy, Physica B **405**, S168–S171 (2010).
[27] B. Náfrádi, A. Olariu, L. Forró, C. Mézière, P. Batail, and A. Jánossy, Phys. Rev. B **81**, 224438 (2010).
[28] A. El-Ghayoury, C. Mézière, S. Simonov, L. Zorina, N. Cobián, E. Canadell, C. Rovira, B. Náfrádi, B. Sipos, L. Forró, and P. Batail, Chem. – Eur. J. **16**, 14051–14059 (2010).
[29] Y. Lakhdar, C. Mézière, L. Zorina, M. Giffard, P. Batail, E. Canadell, P. Auban-Senzier, C. Pasquier, D. Jérome, B. Náfrádi, and L. Fórró, J. Mater. Chem. **21**, 1516–1522 (2011).
[30] B. Náfrádi, Á. Antal, Á. Pásztor, L. Forró, L. F. Kiss, T. Fehér, E. Kováts, S. Pekker, and A. Jánossy, J. Phys. Chem. Lett. **2012**, 3291–3296 (2012).
[31] Á. Antal, T. Fehér, E. Tátrai-Szekeres, F. Fülöp, B. Náfrádi, L. Forró, and A. Jánossy, Phys. Rev. B **84**, 075124 (2011).
[32] Á. Antal, T. Fehér, B. Náfrádi, L. Forró, and A. Jánossy, Phys. Status Solidi B **249**, 1004–1007 (2012).
[33] P. Szirmai, E. Horváth, B. Náfrádi, Z. Mickovic, R. Smajda, D. M. Djokic, K. Schenk, L. Forró, and A. Magrez, J. Phys. Chem. C **117**(1), 697–702 (2013).
[34] P. Szirmai, G. Fàbiàn, J. Koltai, B. Náfrádi, L. Forró, T. Pichler, O. A. Williams, S. Mandal, C. Bäuerle, and F. Simon, Phys. Rev. B **87**, 195131 (2013).
[35] J. Jacimovic, E. Horváth, B. Náfrádi, R. Gaál, N. Nikseresht, H. Berger, L. Forró, and A. Magrez, APL Mater. **1**, 032111 (2013).
[36] M. Choucair, P. Thordarson, and J. A. Stride, Nature Nanotechnol. **4**(1), 30–33 (2009).
[37] B. Náfrádi, R. Gaál, T. Fehér, and L. Forró, J. Magn. Reson. **192**(2), 265–268 (2008).
[38] B. Náfrádi, R. Gaál, A. Sienkiewicz, T. Fehér, and L. Forró, J. Magn. Reson. **195**(2), 206–210 (2008).
[39] P. Szirmai, G. Fábián, B. Dóra, J. Koltai, V. Zólyomi, J. Kürti, N. M. Nemes, L. Forró, and F. Simon, Phys. Status Solidi B **248**(11), 2688–2691 (2011).
[40] M. Choucair, N. M. K. Tse, M. R. Hill, and J. A. Stride, Surf. Sci. **606**(1–2), 34–39 (2012).
[41] R. Blinc, P. Cevc, D. Arčon, B. Zalar, A. Zorko, T. Apih, F. Milia, N. R. Madsen, A. G. Christy, and A. V. Rode, Phys. Status Solidi B **243**(13), 3069–3072 (2006).
[42] M. Galambos, G. Fábián, F. Simon, L. Ćirić, L. Forró, L. Korecz, A. Rockenbauer, J. Koltai, V. Zólyomi, Á. Rusznyák, J. Kürti, N. M. Nemes, B. Dóra, H. Peterlik, R. Pfeiffer, H. Kuzmany, and T. Pichler, Phys. Status Solidi B **246**(11–12), 2760–2763 (2009).
[43] F. Muñoz-Rojas, J. Fernández-Rossier, and J. J. Palacios, Phys. Rev. Lett. **102**(13), 136810 (2009).
[44] M. A. Augustyniak-Jabłokow, K. Tadyszak, M. Maćkowiak, and S. Lijewski, Chem. Phys. Lett. **557**, 118–122 (2013).
[45] K. L. Nagy, B. Náfrádi, N. D. Kushch, E. B. Yagubskii, E. Herdtweck, T. Fehér, L. F. Kiss, L. Forró, and A. Jánossy, Phys. Rev. B **80**(10), 104407 (2009).

